



EURIZON TASK 4.1 Deliverable 4.15

S.M.Liuzzo¹, N.Carmignani², L.Carver, L. Houmami³, T.Perron, S.White⁴,

ESRF, Grenoble France,



I. Agapov⁵, J. Keil⁶, T.Hellert, L.Malina⁷, E.Musa⁸, B. Veglia⁹,

DESY, Hamburg, Germany



ESRF Special Report 01-2023-BD, 15th March 2023.

DESY Special Report, 15th March 2023.

Extract of the document describing EURIZON tasks 4.1:

The beam dynamics studies of the work package 4.1 aim at developing tools and concepts that can be used for the next generation light sources. Existing numerical tools based on the Accelerator Toolbox will be adapted and extended using modern algorithms to provide a framework that could be used during the design and commissioning phases of future storage ring projects or to enhance the performance of existing machines. Developments will focus on methods to improve lattice modeling strategies, perform lattice optimization and correction or simulate realistic operation conditions. The developed tools will be applied to the ESRF-EBS and the PETRA IV lattice models to validate concepts to reduce the natural horizontal emittance or improve the injection efficiency or the lifetime of storage rings. Machine dedicated time at the ESRF or DESY can be allocated for experimental validation when appropriate. Monthly meetings will be organized to follow-up on the progress and share developments.

¹ simone.liuzzo@esrf.fr

² carmignani@esrf.fr

³ lina.houmami@esrf.fr

⁴ simon.white@esrf.fr

⁵ ilya.agpov@desy.de

⁶ joachim.keil@desy.de

⁷ lukas.malina@desy.de

⁸ elaf.musa@desy.de

⁹ bianca.veglia@desy.de





Introduction

The outcome of the discussions during Milestone meetings M4.1.1, M4.1.2 and M4.1.3 has been the definition of the following list of activities

1. Study the impact of magnetic cross talks among neighboring magnets in the H7BA lattice of EBS and H6BA lattice of PETRAIV.
2. Machine Dedicated Time (MDT) experimental activities at EBS and PETRA III for storage ring optimizations:
 - a. Using available optimizers, among which Extremum Seeker¹⁰
 - b. Measurement and analysis of TbT data analysis to determine Storage ring optics
3. Definition of new functions for errors and correction based on pyAT for commissioning simulations of new storage ring projects.

The activities listed above are detailed in the following sections.

Magnetic cross talks for EBS and PETRA IV

To improve storage ring (SR) lattice modeling cross talks should be included in the lattice files at an early stage, before commissioning of the storage ring.

We call cross talk the magnetic field modifications observed when two magnets (either electromagnets or permanent magnets) are at a very short distance (order of the magnets gaps or bore radius, ~50mm for fourth generation light sources) one with respect to the other.

For the EBS storage ring only dipolar cross talk effects were considered initially and no action was taken in terms of lattice modeling. Later, once the SR commissioning started a large tune discrepancy (~1.3 units in the vertical plane) was observed. This discrepancy was solved by introducing quadrupolar cross-talk effect in the lattice^{11,12}. Introducing such an effect in the model earlier would have spared approximately 15 days of commissioning time for EBS; More if this effect would have not been spotted immediately. For future SR light sources such as PETRA IV it is then mandatory to include such effects before commissioning.

In the framework of this project we address cross talks effect in several ways: 1) studies to define an appropriate approach to include cross-talks effect in the lattice model, making use of a minimum number of elements and allowing optics matching; 2) higher order cross-talks, in particular sextupolar cross talks; 3) effect of cross talks in correctors magnets.

¹⁰ A. Scheinker, "Model independent beam tuning", IPAC 2013, TUPWA068

¹¹ <https://link.aps.org/doi/10.1103/PhysRevAccelBeams.24.072401>

¹² <https://link.aps.org/doi/10.1103/PhysRevAccelBeams.24.110701>



Studies to define an appropriate approach to include cross-talks effect in the lattice model

Dipole cross talks are not included in lattice modeling. Their effect has to be considered at the magnet design stage, for example as was done for the EBS lattice, increasing the field of dipole magnets modules close to quadrupoles. When installed the dipole field becomes the nominal one and the quadrupole magnetic center will be measured.

Quadrupole cross-talks are computed by Radia simulations¹³ and have to be introduced in the SR lattice.

The simplest solution is a static-hard-edge model represented by additional fixed field multipoles placed at the correct locations. An example of such a model is visible in Figure 1. Quadrupolar cross talks represented in figure 1 have two effects: one is the generation of some negative quadrupole gradient at the edge of the neighboring dipole, the other is a reduction of the gradient of the quadrupole itself (the field leaked to the dipole). The first effect is modeled in a static-hard-edge model as a thin lens at the side of the dipole. The second effect is a correction factor that must be computed and considered for magnet calibration.

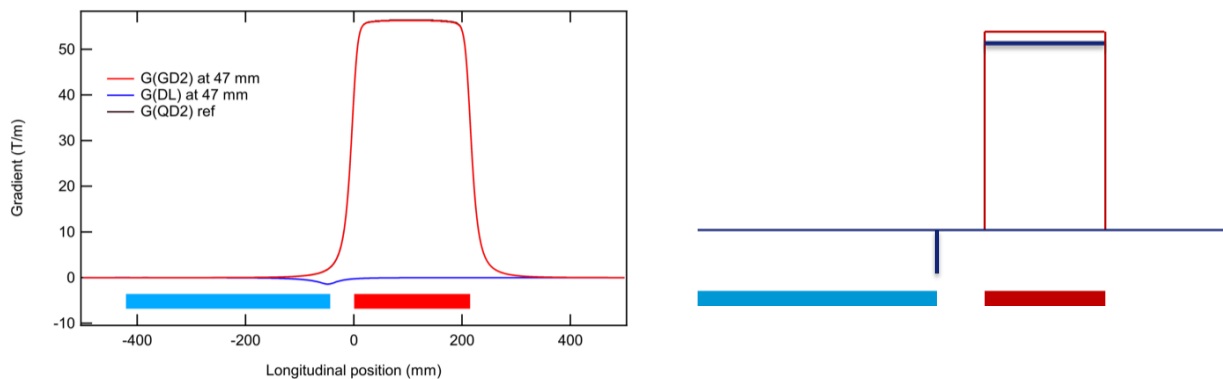


Figure 1: Left: quadrupole-dipole cross talks; Right: static-hard-edge model. The red curves are the field of the quadrupole as if it was far from the dipole. The blue lines represent schematically the field changes to be modeled when the magnets are at their design distance of 47mm.

The additional lenses (18 for the EBS lattice cell, 22 for the injection cell) included in the lattice model imply optics changes that must be compensated by an adequate redefinition of the quadrupole magnets strengths. This process is called optics matching.

With a static-hard-edge model the additional thin lenses do not change their value during the optics matching.

¹³ <https://link.aps.org/doi/10.1103/PhysRevAccelBeams.24.072401>

A first step to improve the optics model would be to link the main magnet quadrupole gradients to their corresponding cross talks effects. When the gradients of the main quadrupoles are varied, so are the cross-talk lenses. This may be easily done in codes such as mad8 and madX. It is less trivial to be done in more modern codes, such as AT¹⁴ and pyAT¹⁵, due to the way in which matching scripts are defined.

A solution proposed towards a dynamic-hard-edge model is a redefinition of the lattice models to a format similar to mad8¹⁶, madX¹⁷, elegant¹⁸, SAD¹⁹, OPA²⁰ and others.

An example is given below:

```
function ring = S28_Longitudinal(Dip, Kquads, Ksext, Koct)

% element definitions
% ...

qf1_1= atmultipole('QF1', 5e-3, 'PolynomB', {1,2}, Kquads(1)*0.01, 'PolynomB', {1,1}, Kdip(1)*0.01);
qf1_2= atmultipole('QF1', 5e-3, 'PolynomB', {1,2}, Kquads(1)*0.2, 'PolynomB', {1,1}, Kdip(1)*0.01);
qf1_3= atmultipole('QF1', 5e-3, 'PolynomB', {1,2}, Kquads(1)*0.5, 'PolynomB', {1,1}, Kdip(1)*0.01);
qf1_4= atmultipole('QF1', 5e-3, 'PolynomB', {1,2}, Kquads(1)*0.7, 'PolynomB', {1,1}, Kdip(1)*0.01);
qf1_5= atmultipole('QF1', 5e-3, 'PolynomB', {1,2}, Kquads(1)*0.9, 'PolynomB', {1,1}, Kdip(1)*0.01);
qf1_6= atmultipole('QF1', 5e-3, 'PolynomB', {1,2}, Kquads(1)      , 'PolynomB', {1,1}, Kdip(1)*0.01);

QF1h = [qf1_1, qf1_2, qf1_3, qf1_4, qf1_5, qf1_6, qf1_6, qf1_6, qf1_6];
QF1 = [QF1h; QF1h(end:-1:1)];

% ...

% build lattice out of blocks
ring = [QF1, Drift, DL, SF2...
]

end
```

This solution, although familiar to the accelerator community and intuitive, is not easily implemented in AT, due to the available matching techniques.

AT matching scripts that make use of the thin lenses already available in the model are under investigation and will be assessed during the project.

Presently the process of implementation of quadrupolar cross-talks in the PETRA IV lattice model is stale, awaiting data from the magnet design.

Since no better modeling has been selected yet, the EBS lattice model has also not been updated and still relies on a static-hard-edge model implementation.

¹⁴ 10.18429/JACoW-IPAC2015-MOPWA014

¹⁵ <https://atcollab.github.io/at/p/index.html>

¹⁶ https://cern.ch/mad8/doc/phys_guide.pdf

¹⁷ <https://www.google.com/search?client=firefox-b-d&q=MADX+guide>

¹⁸ https://ops.aps.anl.gov/manuals/elegant_latest/elegant.html

¹⁹ <https://acc-physics.kek.jp/SAD/>

²⁰ <https://ados.web.psi.ch/opa/>

Higher order cross-talks

Cross-talks concern multipoles of all orders installed in the SR. In the EBS optics sextupoles and octupoles are present. Due to an observed discrepancy among the measured and model chromaticity (about 1% in both planes), the introduction of sextupole cross-talk effects may give at least a partial answer to this issue.

The modelization of sextupole cross-talks in the EBS and PETRA IV models is awaiting for RADIA magnetic model data.

Effect of cross talks in correctors magnets

The design of the magnets for PETRA IV is still ongoing and not all magnet designs exist at the moment. The design work is concentrating on the most demanding magnets which are the quadrupoles of the triplet near the undulators (QD0, QF1, QD2) with large gradients up to 115 T/m and the combined function magnets (DLQ). The combined-function magnets have a longitudinal gradient and are made of permanent magnets. Magnetic field simulations of the three quadrupoles in the triplet are the most advanced and optimized designs exist based on OPERA-3D calculations.

As a first example of the effect of cross-talk between magnets in the PETRA IV lattice the assembly of two quadrupoles QF1 (type PQB) and QD2 (type PQC) and a fast corrector magnet (FC) has been calculated and data were provided by the magnet design group of DESY. The corrector magnet will be installed with equal distance of 79 mm to the yokes of nearby quadrupoles (Figure 2).

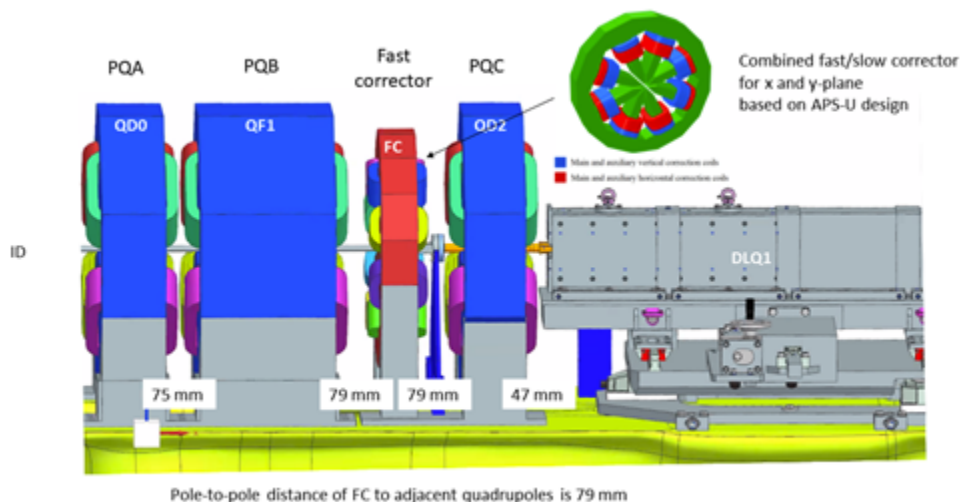


Figure 2: Assembly of a fast corrector (FC) between two quadrupoles (QF1 and QD2) used for cross talk simulations in the quadrupole triplet of PETRA IV.

The corrector magnet has an octupole-like magnet yoke and is based on a design which was developed for APS-U. The corrector magnet combines fast and slow coils for orbit correction in the horizontal and vertical plane and has a better field quality compared to conventional designs using dipole magnets.

The multipole expansion of the B-field as a function of the longitudinal position for five different cases were provided: The two quadrupoles and the corrector alone without any other magnets nearby, the assembly of the three magnets with only the quadrupoles powered and the assembly of the three magnets with all magnets powered. Only the effect of the horizontal slow corrector magnet was simulated and nominal currents were assumed.

The cross-talk reduces the vertical field component of the corrector magnet in the fringe field region and leads to a reduction of the field integral of ~4%. The largest effect occurs near the edges of the nearby yokes of the quadrupoles (figure 3, blue curve, black arrows).

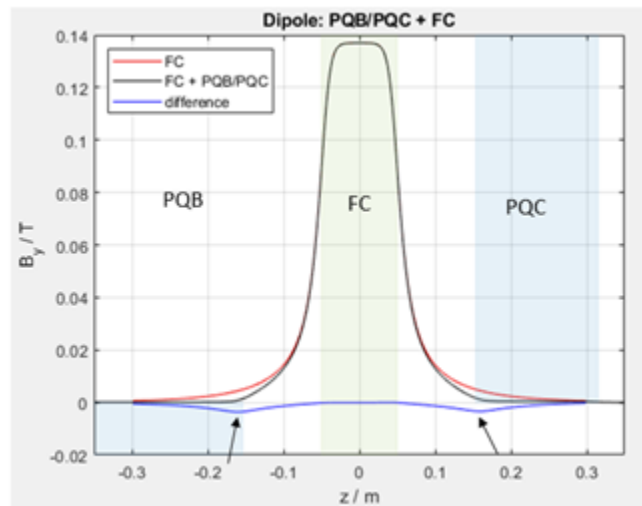


Figure 3: Change of the vertical field component of the corrector without (red) and with the quadrupoles (black). The field difference is shown in blue. Blue and green areas are the hard edge models for the quadrupoles and corrector magnets.

A simple model to take the cross-talk of the corrector magnet into account would be the use of a hard-edge model with a corrected calibration curve and two zero-length correctors with negative dipole field integrals at the edges of the quadrupoles.

The change of the quadrupole gradients due to the excitation of the fast corrector is shown in Fig. 4. It can be seen that the cross talk reduces mainly the gradient of PQC (nearly 1%) while the gradient of the PQB quadrupole is mostly unaffected. Different saturation of the quadrupoles could be the reason for this. In addition, changes of the gradient appear near the edges of the yokes of the quadrupoles and the corrector.

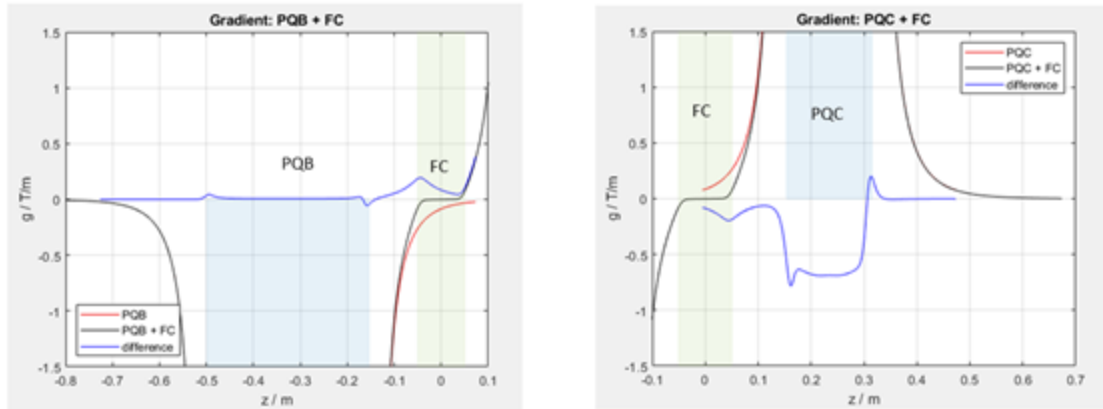


Figure 4: Change of the gradients of the quadrupoles without (red) and with the fast corrector (black). The difference of the gradient is shown in blue. Left picture for PQB, right picture for PQC. Blue and green areas are the hard edge models for the quadrupoles and the corrector magnet.

For the two quadrupoles the effect of the cross-talk could be modeled by using a hard edge field approximation of the quadrupoles with a corrected calibration curve and several zero-length quadrupoles with negative integrated gradients at the edges of the quadrupoles and the corrector.

These simple models – although not perfect - would already be useful to take cross-talks into account and would help to improve the lattice model of PETRA IV. A better agreement could be achieved by using the measured longitudinal distribution as it was described in the previous section.

Further steps

The work done above and in the future of this project concerning cross talks will also benefit any other lattice upgrade that foresees installing magnets very close to each other. The application of common schemes to two different light sources, forces the development to be as general as possible, thus leading to more versatile solutions that may be adopted also by other existing or planned SR.

MDT activities at EBS and PETRA-III for storage ring optimizations

Common MDT activities are planned at the EBS and PETRA-III storage ring to target optimization and determination of machine parameters. The measurement and optimization techniques used are adapted from existing ones and point to develop and enforce the use of sharable tools among several facilities.

Machine Dedicated Time (MDT) for experimental activities at EBS and PETRA III has been allocated until January 2023:

- lifetime and vertical emittance optimizations using Extremum Seeker²¹
- Measurement and analysis of TbT data analysis to determine Storage ring optics

Lifetime optimizations using extremum seeker

Summarized description of the optimizer

The Extremum Seeker (ES) is a local, model-independent algorithm²². It requires a cost function which may be analytically unknown $\hat{C}(p, t)$, but which depends on accelerator parameter settings and must be maximized or minimized. The algorithm adjusts the parameters p_j according to

$$\frac{dp_j}{dt} = \sqrt{\alpha\omega_j} \cos\left[\omega_j t + k\hat{C}(p, t)\right]$$

Where $\alpha > 0$ is the dithering amplitude, the frequencies $\omega_j = \omega r_j$ and $r_j \neq r_i$ for $i \neq j$. The term $k > 0$ is the feedback gain. In case of maximization k is chosen negative.

Implementation begins by setting parameter values to some initial conditions, $\mathbf{p}(1)$, recording the cost function $C(1)$, and then performing the update:

$$p_j(2) = p_j(1) + \Delta\sqrt{\alpha\omega_j} \cos\left[\omega_j\Delta + k\hat{C}(p, t)\right]$$

with $\Delta = 2\pi/(10 * \max\{\omega_j\})$ being the discrete time step small enough so that the finite-difference approximation of ES dynamics is accurate with the highest frequency component requiring at least 10 steps to complete one full oscillation.

The algorithm was adapted from the existing version implemented in the Ocelot simulation toolkit (https://github.com/ocelot-collab/optimizer/tree/master/op_methods).

ES, with its ability to handle open-loop unstable, time-varying, nonlinear systems, is an ideal candidate for online persistent control and optimization of complex, many parameter, large systems. Because the dynamic feedback for stabilization and optimization is

²¹ A. Scheinker, "Model independent beam tuning", IPAC 2013, TUPWA068

²² A. Scheinker and M. Krstić, "Minimum-Seeking for CLFs: Universal Semiglobally Stabilizing Feedback Under Unknown Control Directions," in *IEEE Transactions on Automatic Control*, vol. 58, no. 5, pp. 1107-1122, May 2013, doi: 10.1109/TAC.2012.2225514.

model-independent, can tune multiple parameters simultaneously and is robust to measurement noise, it has gained popularity in particle accelerator applications, since accelerators are usually very large complex systems with many magnet components and time-varying beam distributions. This method has been applied to accelerators around the world including adaptive online model tuning for non-invasive electron beam diagnostics at the Facility for Advanced Accelerator Experimental Tests (FACET) at SLAC National Accelerator Laboratory²³.

Work done to prepare the MDT

The algorithm was first tested on a simple cost function (plotted below in figure 5) varying the hyperparameters (k_{ES} and α) to understand their impact on the optimization routine.

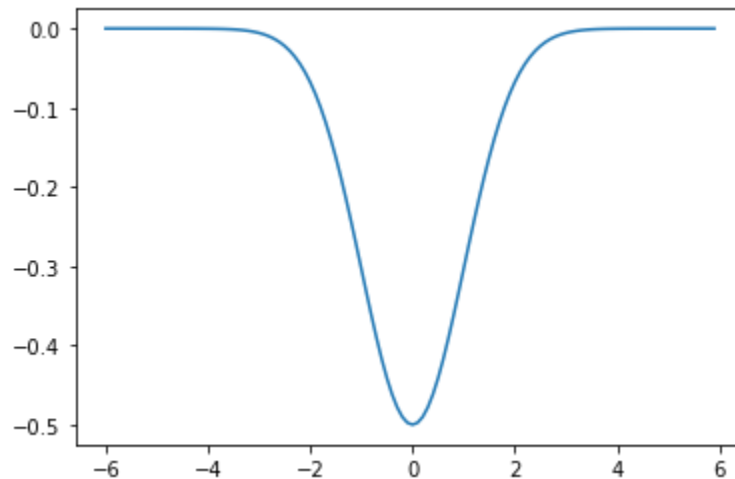


Figure 5: simple example of cost function used to test the ES algorithm code.

Increasing the value of k_{ES} leads the routine to converge towards the minimization of the simple cost function chosen as example (see figure 6).

²³ Scheinker, Alexander, and Spencer Gessner. "Adaptive method for electron bunch profile prediction." in *Physical Review Special Topics-Accelerators and Beams* 18.10 (2015): 102801. <https://doi.org/10.1103/PhysRevSTAB.18.102801>

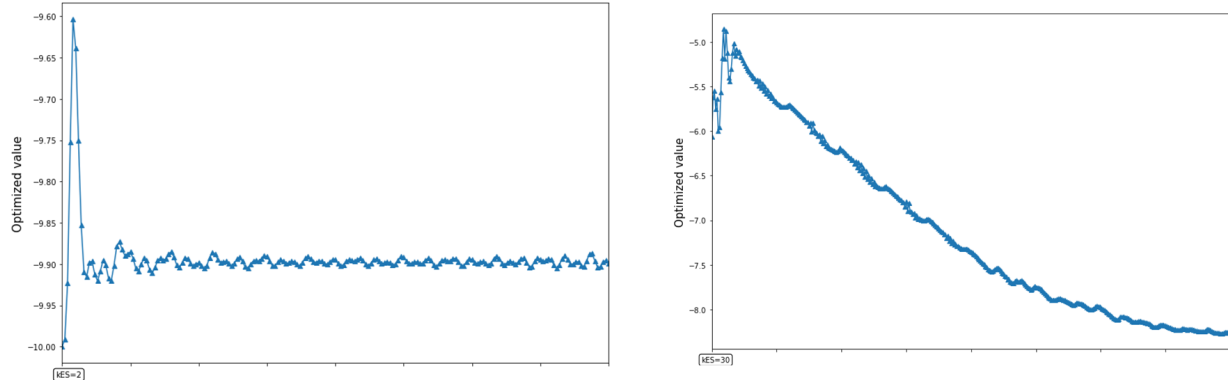


Figure 6: evolution of the example cost function during the minimization routine with two different values of $k_{ES}=2$ (left) and $k_{ES}=30$ (right).

Successively the ES optimizer was tested in pyAT²⁴ simulations for the EBS storage. The chosen target of the simulated optimization is minimum vertical emittance. Two cases were addressed. In the first case the vertical emittance was increased intentionally setting a random value for the skew quadrupole strength of a single skew quadrupole (on an SF2 sextupole). In the second case all skew quadrupoles were set to random values. The ES algorithm was used in both cases to minimize the vertical emittance calculated by the pyAT program. The variables used for the minimization were 32 skew quadrupole strengths of the SF2A family.

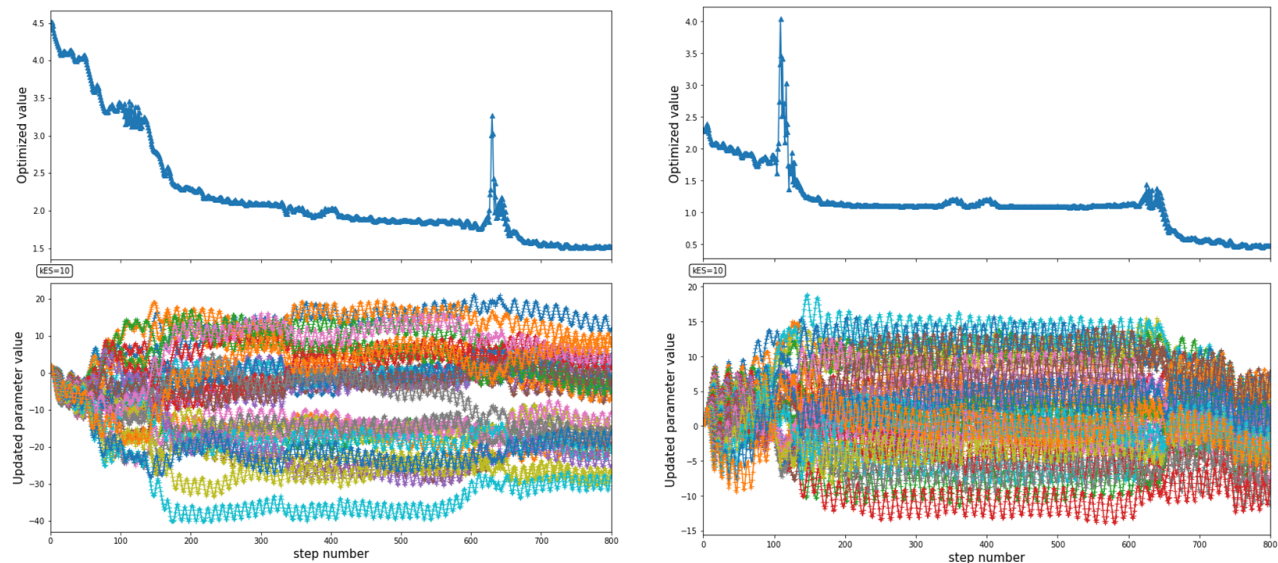


Figure 7: Left: only one skew quad of the SF2A in the pyAT simulated lattice is excited to induce an increase on the vertical emittance (optimized value, top) which is minimized by the ES algorithm tuning 32 SF2A knobs (updated parameter value, bottom). Right: all the skew quads are excited and compensated with the same knobs as left.

In the first case ES was expected to find exactly the value of the single magnet moved. In the second case there was no particular expectation on the pattern of corrections. Figure 7 shows

²⁴ <https://atcollab.github.io/at/p/index.html>

the result of these 2 simulated optimizations scenarios. In both cases the ES optimizer finds an improved solution for the vertical emittance.

Other tests in preparation of the MDT were performed also using the EBS control system simulator²⁵. Several features were added to the ES algorithm to improve its user-friendliness:

- Updated figures which plots the evolution of the minimized value(s) and the sent amplitudes contained in the vector x with the number of iterations (e.g. Fig. 7),
- A data saving function in python which includes the correction strengths of the skew quadrupoles for testing in the ESRF-EBS storage ring.

Description of the MDT activity

Following the promising simulations, the ES algorithm was tested on the ESRF-EBS storage ring during a four-hour machine dedicated time (MDT) on November 28th 2022. As proof of principle and to work on a low-current beam, the ES was adapted to the vertical emittance minimisation tested in simulation rather than lifetime optimizations (the final target of these studies). The waiting time, added to ensure the skew quadrupoles arrive at the requested strengths and that the read value of the vertical emittance has stabilized, is set to 5 seconds.

The plan of the MDT was as follows:

1. Vertical emittance minimisation : first test
 1. Detune **ONE SF** skew quadrupole
 2. Save SRMagnet file
 3. Scan the parameters
 4. Try the ES algorithm with 32 SF skew including the detuned one.
 5. Save the SR Magnet file
 6. Compare the vertical emittance before and after
2. If satisfactory,
 1. Send random errors in the skew quadrupoles
 2. Save SR Magnet file
 3. Scan the parameters
 4. Try the ES algorithm with 32 SF skew.
 5. Save the SR Magnet file
 6. Compare the vertical emittance before and after

The ESRF-EBS electron beam has a low equilibrium vertical emittance of 0.5 ± 0.1 pm.rad.

The Extremum Seeking algorithm was run through a Jupyter notebook in the ESRF-EBS control room. The MDT started with the introduction of a $+0.005$ m⁻¹ correction strength in **one skew**, located at a sextupole of the SF2A family (see Fig. 8), which increases the vertical emittance to 3.9 ± 0.1 pm.rad. The minimisation will be conducted using all the 32 skew quadrupoles located at the SF2A sextupoles.

²⁵ S.Liuzzo et al. "The EBS simulator: a commissioning booster"
[10.18429/JACoW-ICALEPCS2021-MOPV012](https://doi.org/10.18429/JACoW-ICALEPCS2021-MOPV012)

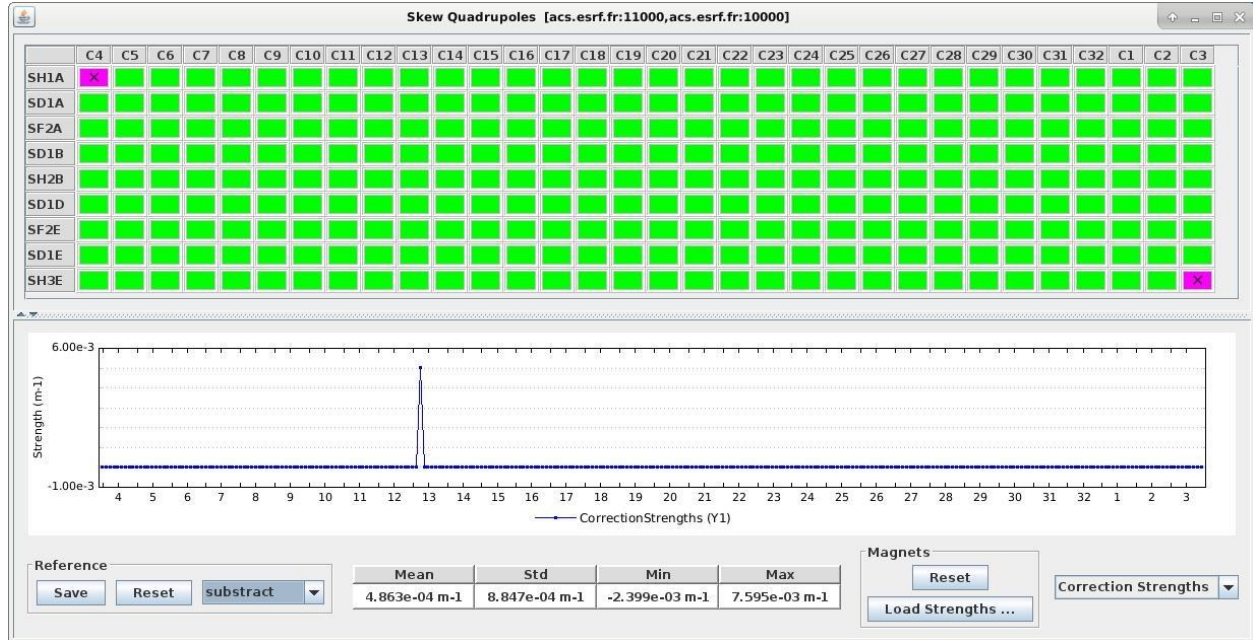


Figure 8: Skew quadrupole correction strengths at the beginning of the MDT. The application shows the difference between the current strengths and the nominal strengths.

The first minimisation is launched with the standard hyperparameters $\alpha = 3 \cdot \alpha_0$ and $k_{ES} = 40$ which provided a good response in simulations. The result of the first 70 iterations as well as the sent amplitudes are displayed in Fig. 9 left. Two limitations are spotted: the amplitudes reach too large values, and the first observed reduction from 3.9 to 2.9 pm.rad is not aggressive enough to ensure a fast minimisation. Therefore, the boundaries were decreased from $[-8;8]$ to $[-5;5]$, and k_{ES} decreased to 30 to limit the impact of the read emittance value in the perturbation function. The results are displayed in Fig. 9 right. The conducted changes are followed by small variations in the vertical emittance around the starting point. This minimisation was stopped when the emittance blew up with increased amplitudes of the skew quadrupole strengths. The first step was not successful: first, the very localized error on one skew, although simple to correct, still triggers a global response of the selected knobs. Then, it appears the ES algorithm loses knowledge of the previous found minimum and struggles to go back. The time constraints of the MDT as well as the duration of each ES run forced us to move on with the tests.

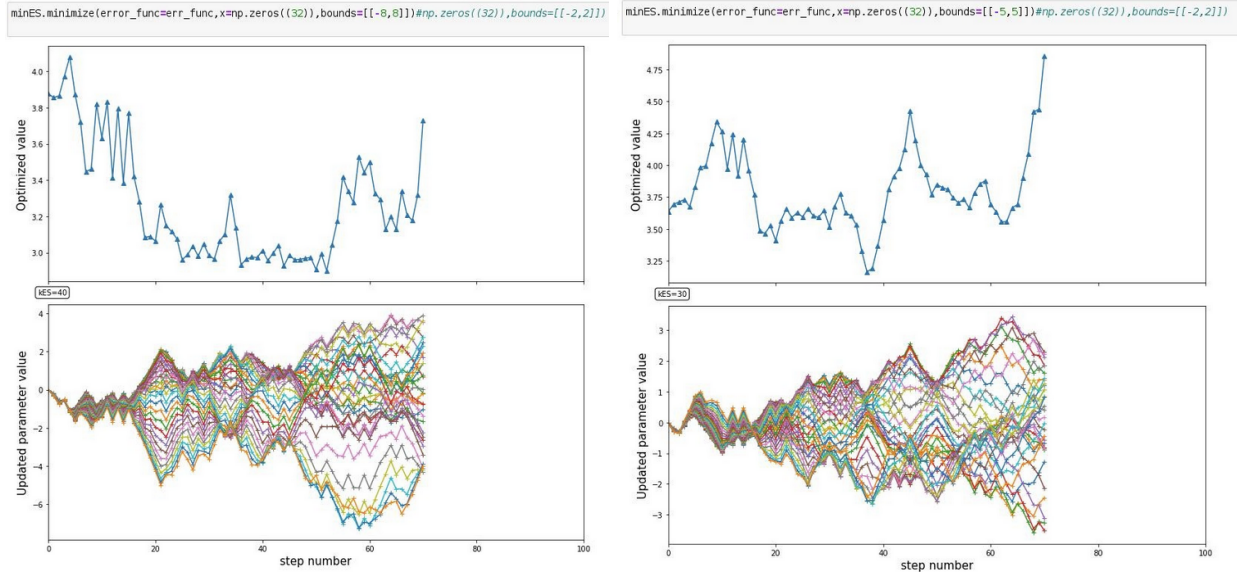


Figure 9: Evolution of the vertical emittance (top figures) and amplitudes sent to the skew quadrupoles on the SF2A during two Extremum Seeking sessions (left) with $\alpha = 3\alpha_0$, bounds = $[-8;8]$ and $k_{ES} = 40$ and (right) $\alpha = 3\alpha_0$, bounds = $[-5;5]$ and $k_{ES} = 30$.

Instead of perturbing one skew, we sent random errors to all skew quadrupole, limited to 1% strength change, which generated a vertical emittance of 5.7 pm.rad. The next ES run used the same hyperparameters as the latest run, and the same knobs. The variation in vertical emittance were of the 10^{-3} order, so the parameter α was increased to $6\alpha_0$. Figure 10 illustrates the variation of the emittances at the beginning of this minimisation.

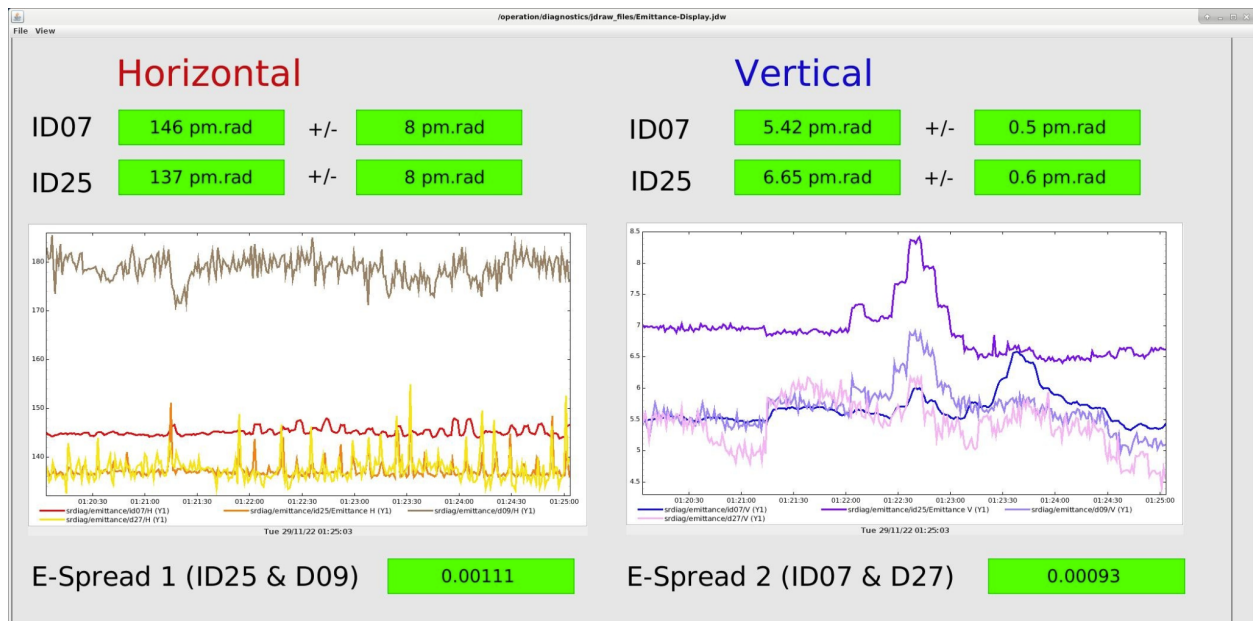


Figure 10: Emittance measurements in the ESRF-EBS storage ring during the first iterations of

an ES minimisation of parameters $\alpha = 6 \cdot \alpha_0$, bounds = [-5:5] and $k_{ES} = 30$. The emittances are calculated at two pinholes in the SR. The reference is measured in ID07, which corresponds to the red and blue lines for the horizontal and vertical emittances respectively.

Despite presenting small and promising variations in the vertical emittance, this minimisation ended with large amplitudes in the skew quadrupoles exceeding the input boundaries, and a blow up of the emittance from 5 pm.rad to about 30 pm.rad, as seen in Fig. 11. This phenomenon is to be avoided in a future version of the algorithm, with for instance a control on the maximum emittance allowed with a restoration to a previous minimum.

```
minES.minimize(error_func=err_func, x=np.zeros((32)), bounds=[-5,5])#np.zeros((32)), bounds=[-2,2]]
```

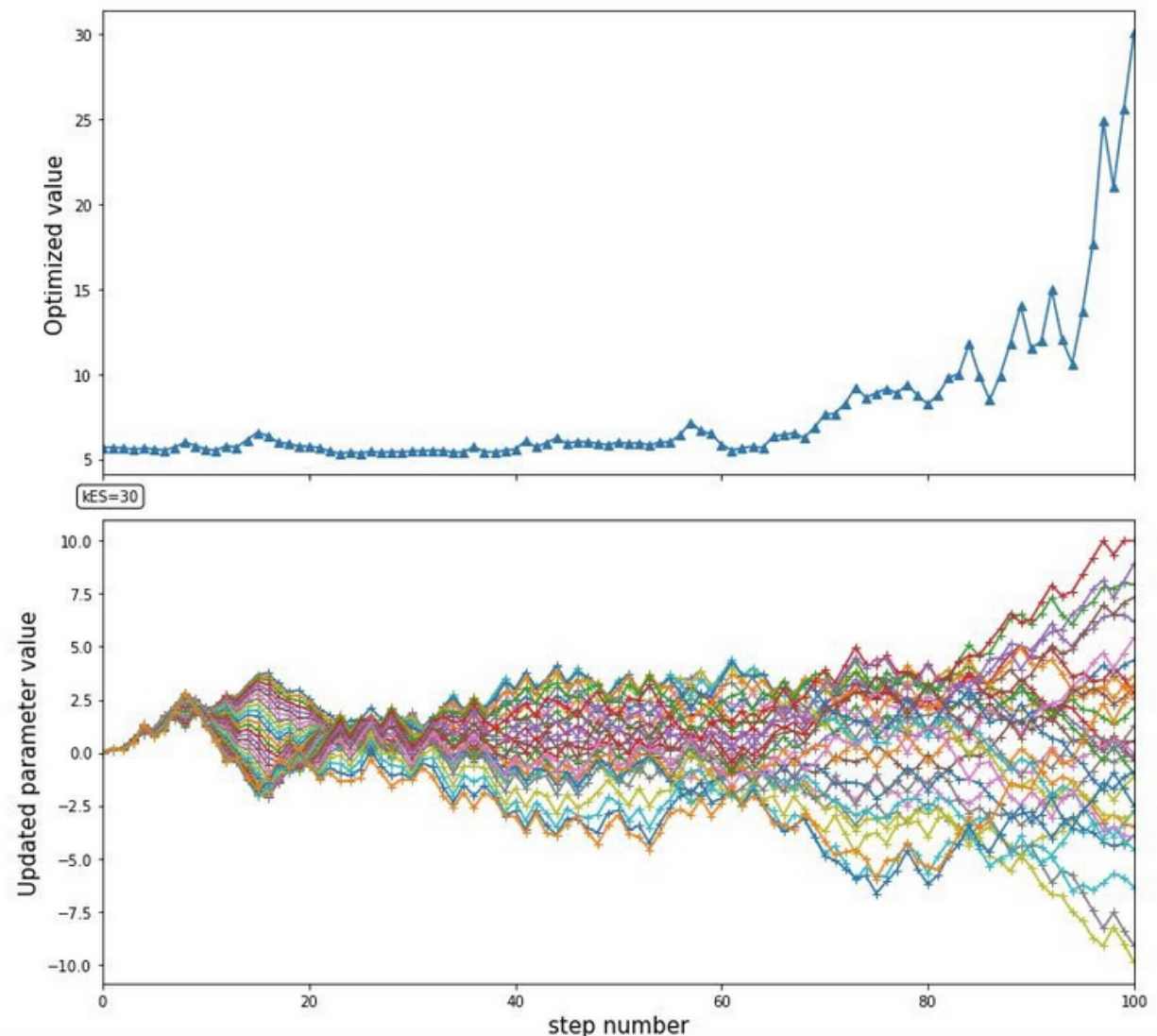


Figure 11: ES minimisation of parameters $\alpha = 6 \cdot \alpha_0$, bounds = [-5:5] and $k_{ES} = 30$.

A last test drastically reduced the boundaries on the amplitudes to $[-1;1]$ and increased k_{ES} to 40 to start a minimisation sooner, and reduced $\alpha = 2 * \alpha_0$ to slow down the amplitude variations. The previous skew quadrupole corrections are replaced with new small (less than 1% variation) random strengths, for a vertical emittance of 5.8 pm.rad. The evolution of the amplitudes and vertical emittance during this minimisation is in Fig. 12. The boundaries were respected and triggered a stronger minimisation after the 200 step. The minimisation ended after reaching its maximum iteration number which resulted in a total emittance reduction of 1.2 pm.rad.

```
minES.minimize(error_func=err_func,x=0.2*np.ones((32)),bounds=[[-1,1]]#np.zeros((32)),bounds=[[-2,2]
```

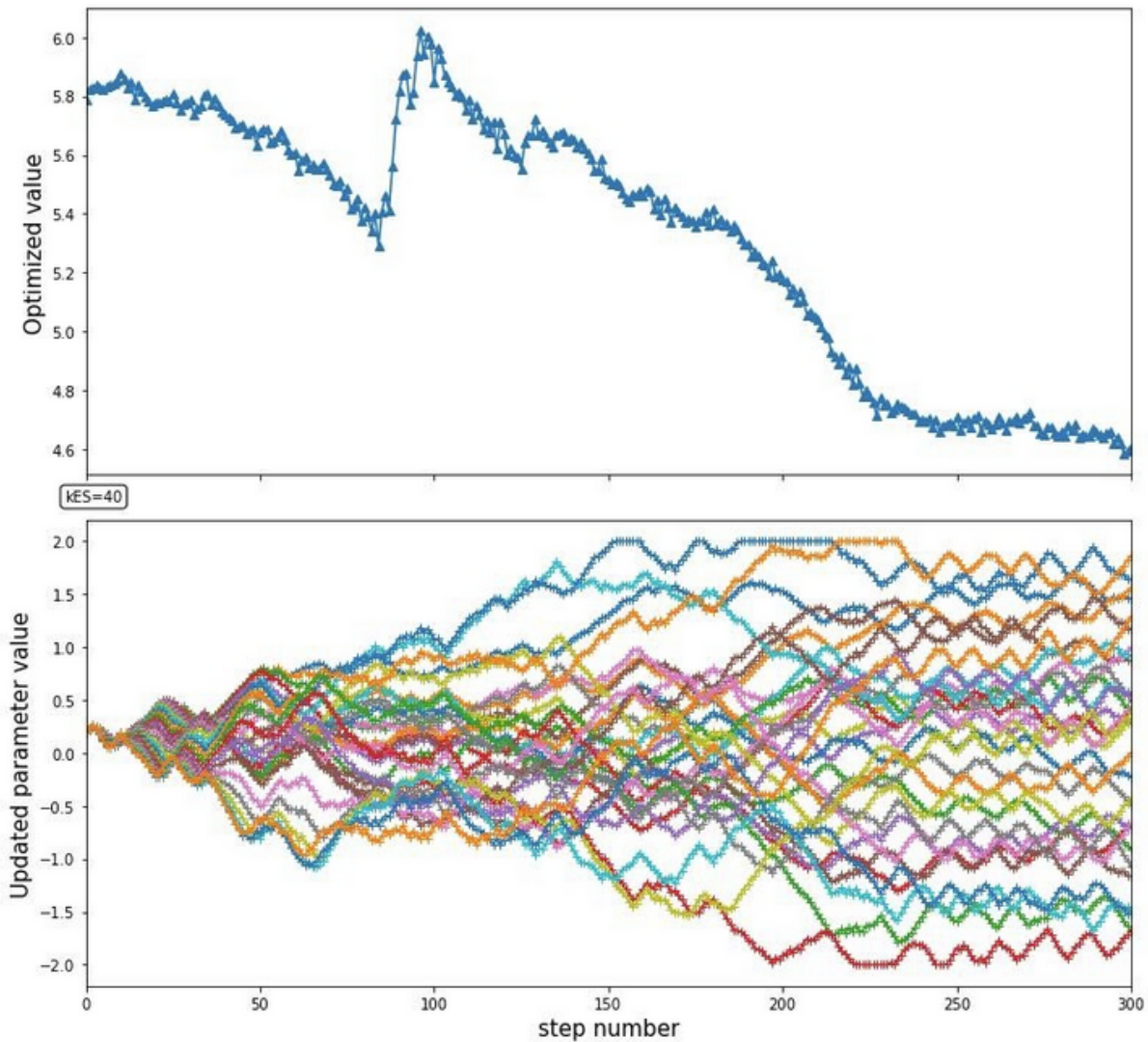


Figure 12 : ES minimisation of parameters $\alpha = 2 * \alpha_0$, bounds = $[-1;1]$ and $k_{ES} = 40$.

Results and outlook

The vertical emittance minimisation study of the ES algorithm on the ESRF-EBS storage ring had limited results. Firstly, a long time is required to select the hyperparameters of the ES, and a simple scan is not efficient. Future simulations should aim at reducing the time allocated for the hyperparameter selection. Secondly, a 20% reduction of the emittance was achieved after 30 minutes, with no convergence of the algorithm. To make the algorithm more robust and avoid stagnation to local minimum, an evaluation of the convergence during the minimisation could be implemented. This additional module would estimate a possible local minimum and modify the hyper-parameter α to increase the amplitude of the perturbation and scan a larger scale, and increase k_{ES} to increase the impact of the cost function on the parameter update. This could speed up the convergence and make the ES a more time-efficient algorithm.

Provided further simulations dedicated to lifetime optimisation, a future MDT could be planned using an improved version of Extremum Seeking algorithm or different tools, such as Badger²⁶. It would then be compared to the current lifetime optimisation conducted on the ESRF-EBS after each shutdown of the accelerators²⁷. The provisional plan of that MDT is available in Appendix.

Measurement and analysis of TbT data analysis to determine Storage ring optics

The correction of the linear optics is very important to operate the synchrotron light sources reliably, with good lifetime and good injection efficiency. Most of the light sources measure the linear optics and compute the corrections by fitting the orbit response matrix (ORM). This is a standard technique and it is used both at the ESRF and at DESY.

Alternatively to the orbit response matrix measurement, the linear optics can be obtained from the analysis of the turn-by-turn (TBT) signals from the beam position monitors (BPMs) when the beam is excited with an oscillating dipole magnet (AC-dipole). This technique is used in colliders as LHC²⁸ but also in some light sources, as PETRA-III in DESY²⁹.

Turn by turn data with betatron oscillations can be obtained with a single turn kicker. In that case, the oscillations become quickly decoherent because of non zero chromaticity and non zero detuning with amplitude. If the decoherence is small, because the chromaticity and the detuning with amplitude are small, the oscillations are damped by the synchrotron radiation in a few tens of ms. The TBT and ORM methods were compared in ESRF's predecessor of EBS.

An AC-dipole can create a stable oscillation at large amplitude without decoherence.

²⁶ Zhe Zhang, <https://github.com/slaclab/Badger>

²⁷ N. Carmignani, et al., Online Optimization of the ESRF-EBS Storage Ring Lifetime, Proceedings of IPAC22, Bangkok, Thailand, 2022, doi = 10.18429/JACoW-IPAC2022-THPOPT001

²⁸ R.Thomas, LHC optics measurement and correction software progress and plans, <https://doi.org/10.18429/JACoW-IPAC2019-WEPGW116>

²⁹ A.Kling, Turn-by-turn data analysis for PETRA-III, IPAC 2010, WEPEA017

Optics measurements with TBT analysis of the oscillations driven by an AC-dipole have the advantage to be much faster than the orbit response matrix measurement. The precisions obtained with the two techniques are comparable.

Work done to prepare the MDT

A magnetic shaker is installed in the ESRF storage ring and it is used to blow-up the emittance of the beam using a white noise. The AC-dipole excitation is obtained by sending a sinusoidal signal at a specific frequency, close to the betatron tune, to the magnetic shaker. The magnetic shaker used as an AC-dipole has been tested before the MDT.

A procedure to switch the BPM to TBT acquisition mode has been prepared by the diagnostics group and has been tested before the MDT. The aim of this procedure is that the BPMs are all synchronized and don't mix the signal from two consequent turns.

The Optics Measurements and Corrections (omc3³⁰) python code to do the analysis has been developed at CERN and is used in several machines, for example, at PETRA III. Before the MDT, the code has been installed at ESRF and it has been tested in simulations. The ESRF lattice has been converted in MAD-X format to be compatible with the omc3 code. The analysis parameters of the ESRF lattice have been defined within omc3 and are subject to further tuning.

Description of the MDT activity

An MDT shift on November 7th 2022 was booked to try the analysis of the TBT signal with the AC-dipole at the ESRF.

The amplitudes and frequencies of the AC-dipole were tuned to have a good TBT signal, similar to the ones tested in simulations.

The filling pattern of the machine had to be short enough in order to avoid issues with BPM synchronization and to limit the excitation phase difference for the different bunches (see fig. 13). With 100 bunches, the phase difference inside the train was considered negligible.

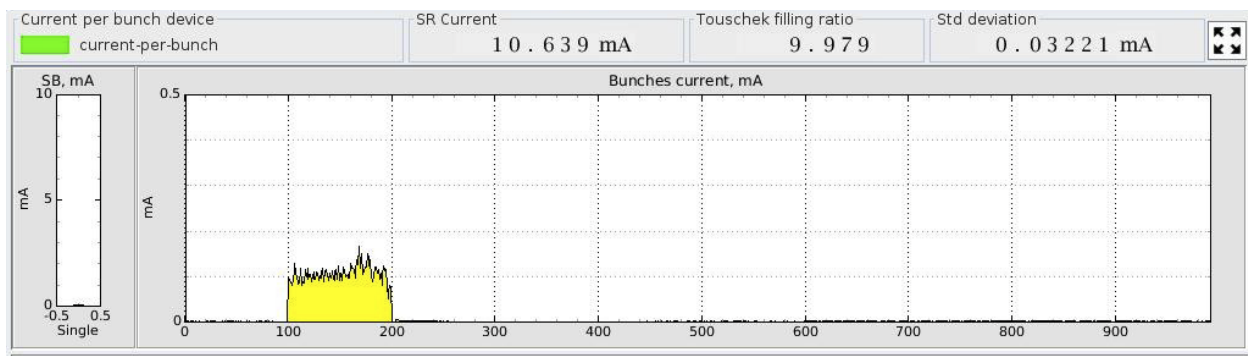


Figure 13: Filling pattern used in the ESRF storage ring for the AC-dipole MDT.

³⁰ <https://github.com/lmalina/omc3>

The TBT data were acquired for about 50000 turns and many different acquisitions were performed, varying the total current, the filling pattern, the amplitude and the frequencies of the excitation.

In the currently best conditions, the beta functions could be measured from the frequency analysis of the TBT data with about 5 to 10% error rms (Fig. 14). This is still not at the acceptable level, so more studies have to be performed to better understand the reasons for the low accuracy. Certainly, the analysis parameters have to be optimized for the ESRF lattice.

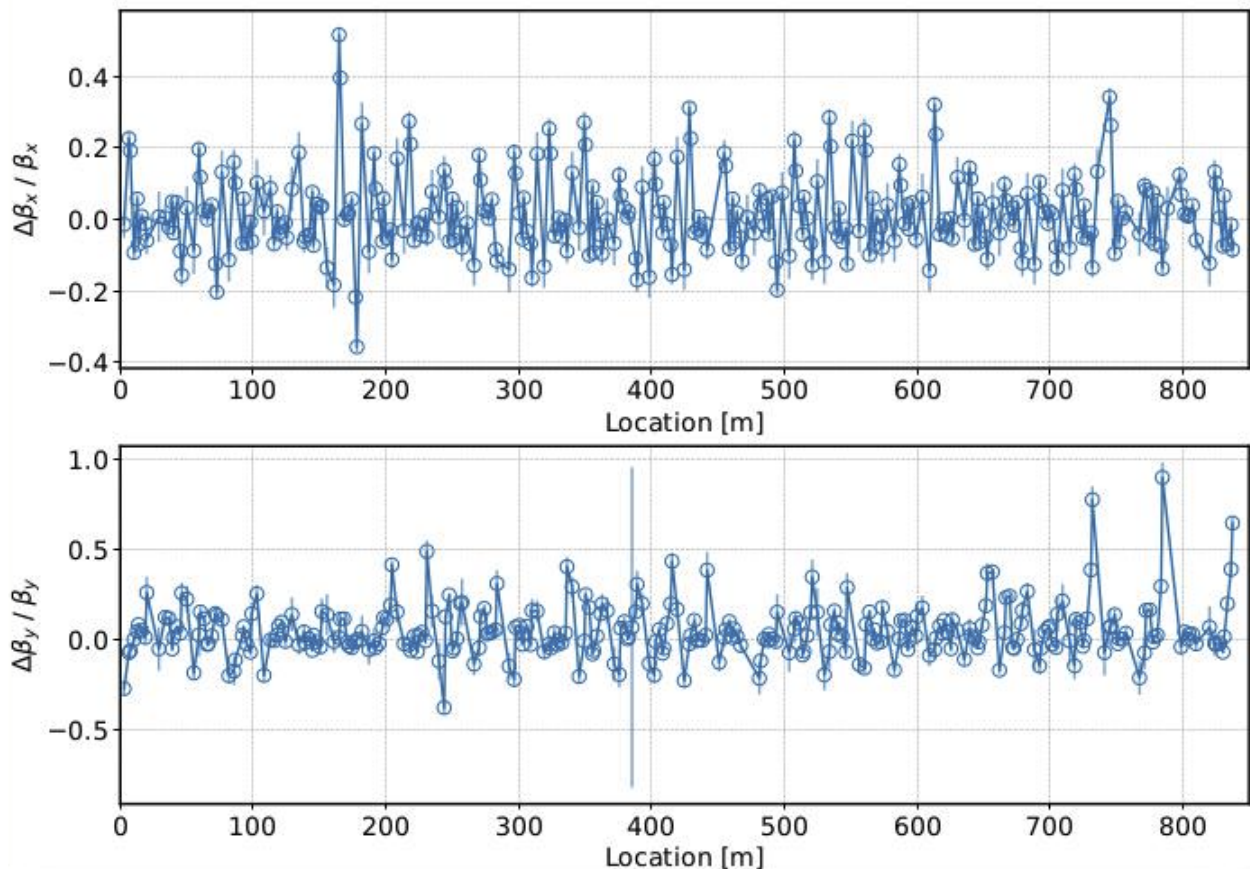


Figure 14: Beta beating measurement with TBT analysis.

Results and outlook

The accuracy of the measurement of the beta function at the ESRF with the analysis of the BPM TBT signal with AC-dipole excitation is currently not at the level of the orbit response matrix, so further studies (both in simulation and experimental) are planned to better understand the problem.

A new MDT in Petra III is planned to further develop TBT-data-based methods.

Definition of a new functions for errors and correction based on pyAT

Commissioning simulations are mandatory for any new storage ring (SR) design. Running such simulations allows to define the procedures to achieve first turns, accumulation and finally low emittance tuning and optics corrections. Once all the correction steps are tuned and optimized these commissioning simulations show if the SR under study will be able to reach its design performance in terms of injection efficiency (IE) and Touschek lifetime (TL). Commissioning simulations are thus mandatory for any SR not only to define the final performances in presence of realistic errors but also to evaluate maximum tolerated errors, to chose the optimal commissioning correction sequences and to asses the loss/gain in DA, IE, TL of optics adaptations performed while operating the SR.

Tools for commissioning simulations are available based on several codes (among others see ³¹ and ³²), but it is often difficult to adapt to other SRs. Recently Simulated Commissioning (SC)³³ has been introduced to the community based on matlab accelerator toolbox (AT)³⁴.

Work has been carried out in the framework of the present project to provide a set of tools for commissioning simulations also for the python version of AT.

Implementation of a pyAT based commissioning simulation toolkit

The actions expected from a commissioning simulation toolkit are rather basic:

- 1) set errors based on a given error table to generate N possible realistic SR scenarios
- 2) correct lattice
- 3) compute relevant quantities (DA, IE, MA, etc...)
- 4) visualize a summary of the results

The software tools developed (available for download here:

<https://gitlab.esrf.fr/BeamDynamics/commissioningsimulations>) are designed considering also the following specifications:

- simple definition of errors and corrections to apply: python dictionaries.
- Modular structure (each component of the code is stand-alone. Other parts of the code may be added easily, as plugins)
- Tests / example / demos available for each submodule and for the overall usage
- Parallel computation (multiprocessing)

³¹ S. Liuzzo, N. Carmignani, J. Chavanne, L. Farvacque, G. Le Bec, B. Nash, P. Raimondi, R. Versteegen, S. White, "Updates on Lattice Modeling and Tuning for the ESRF-EBS Lattice.", 7th International Particle Accelerator Conference, 10.18429/JACoW-IPAC2016-WEPOW005, WEPOW005, 2016

³² Sajaev, V., "Commissioning simulations for the Argonne Advanced Photon Source upgrade lattice", PhysRevAccelBeams.22.040102, 10.1103/PhysRevAccelBeams.22.040102

³³ T. Hellert, C. Steier, M. Venturini "Lattice correction and commissioning simulation of the Advanced Light Source upgrade storage ring" PhysRevAccelBeams.25.110701, 10.1103/PhysRevAccelBeams.25.110701

³⁴ B.Nash, N. Carmignani, Farvacque, S. Liuzzo, T. Perron, P.Raimondi, R. Versteegen, S. White, (2015). NEW FUNCTIONALITY FOR BEAM DYNAMICS IN ACCELERATOR TOOLBOX (AT)

- SLURM cluster submission (parallel / distributed computations)
- Organized folders, easy to add seeds, easy to retrieve data
- Possible to skip/postpone DA/MA for correction loop optimization
- 6D tracking, with radiation and RF cavity managed by pyAT
- use of analytic / semi-analytic / numeric computations
- flexible to changes of SR (centralized input of all machine dependent parameters)
- flexibility in the definition of the corrections to be applied
- speed of computations, making use of analytic formulas where possible
- easy python installation “pip install .”

A single configuration file holds all the lattice dependent information. This includes for example the location of correctors required for each step of the correction.

A flag is used to switch between local and cluster computing. In the first case lattices are analyzed in series, and computations are done exploiting all available local computing resources. In the second case, a given number of processors is charged to analyze the N lattice seed. In this case also the lattice seeds are analyzed in parallel. The two options are kept in order to make the code usable also by laboratories where large computing clusters are not available. Figure 15 shows the code running in local mode or in cluster mode.

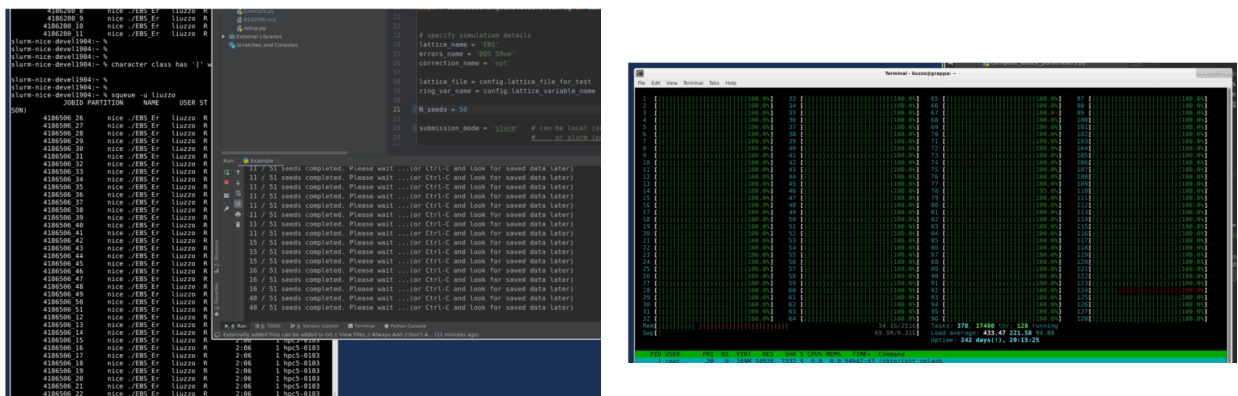


FIGURE 15: pyAT based software running (right) in a local 128 cores machine or (left) using a remote computing cluster.

The data produced by the code is organized in subfolders as depicted in Fig 16

```
├── Design # FOLDER of data for reference Lattice
│   ├── DATLTDesign.pkl # data of DA and LT
│   ├── DADesign.png # DA image
│   ├── LatticeDesign.pkl # pyAT lattice file
│   ├── TLTDesign.png # MA image
│   └── LatticeDesignData.pkl # optics parameters file
├── Matrices # FOLDER of data for response matrices
│   ├── TRM.mat # trajectory response
│   ├── ORM.mat # orbit response
│   ├── Jnumeric.mat # derivative of ORM for optics correction
│   └── ...
├── Seed000 # FOLDER of data for Seed000
│   ├── Errors.pkl # errors assigned to this Seed 0
│   ├── Errors.txt # printed version of errors assigned to seed 0
│   ├── LatticeErrors.pkl # pyAT lattice with errors in key rerr
│   ├── LatticeErrorData.pkl # optics parameters file for lattice with errors
│   ├── LatticeCorrected.pkl # pyAT lattice with errors and correction in key rcor
│   ├── LatticeCorrectedData.pkl # optics parameters file for lattice with errors and correction
│   ├── DAErrors.png # DA image
│   ├── DATLTDerrors.pkl # data of DA and LT with errors
│   ├── TLEErrors.png # MA image with errors
│   ├── DACorrected.png # data of DA and LT with errors and corrections
│   ├── DATLTCorrected.pkl # data of DA and LT with errors and correction
│   ├── DA_compare.png # DA image comparing design, errors and errors+correction
│   ├── TLTCorrected.png # MA image with errors and correction
│   ├── ComparativeData.pkl # data compared to Design
│   ├── ComparativeData.txt # printed version of data compared to Design
│   └── MA_compare.png # MA image comparing design, errors and errors+correction
├── Seed002
├── Seed003 # same structure as Seed000 folder
├── ...
├── Seed##
├── CorrectionParameters.pkl # global correction parameters
├── params.txt # slurm submission file of parameters
├── sbatch.sh # slurm submission file
├── SummaryFigures # FOLDER of figures summarizing the above data
│   ├── DA.png
│   ├── LT.png
│   ├── MA.png
│   ├── Beta.png
│   ├── COD.png
│   ├── DISP.png
│   ├── EMIT.png
│   └── TUNE.png
```

Figure 16: pyAT commissioning simulations output folders structure. One folder per seed is present and one folder with the reference design values.

In order to speed up the tests, and in particular to choose and fine tune the correction scheme it is not necessary to compute DA, IE and MA. It is sufficient to look at basic lattice optics parameters such as orbit, tunes and optics. For this reason, the computation of DA, IE and MA may be excluded, with a significant gain in time (up to more than 90%).

All features of the pyAT tracking engine are inherited by the software. Full 6D tracking of electrons in presence of radiation, quantum diffusion and RF cavities may be performed by simply setting appropriately the input lattice.

Error setting is also based on the core pyAT. For the moment only the basic errors (alignment, gradient, rotation and BPM errors) are available, but work is ongoing on this topic and will be part of the next report.

Correction using pyAT based commissioning simulation toolkit

The corrections available and tested are presently:

- First turns beam threading³⁵ (see Figure 17)
- closed orbit correction
- tune correction
- chromaticity correction
- error model fit based on closed orbit response matrix (LOCO like optics correction)
- optics correction³⁶ (see Figure 18)
- coupling correction
- normal and skew quadrupoles RDTs correction

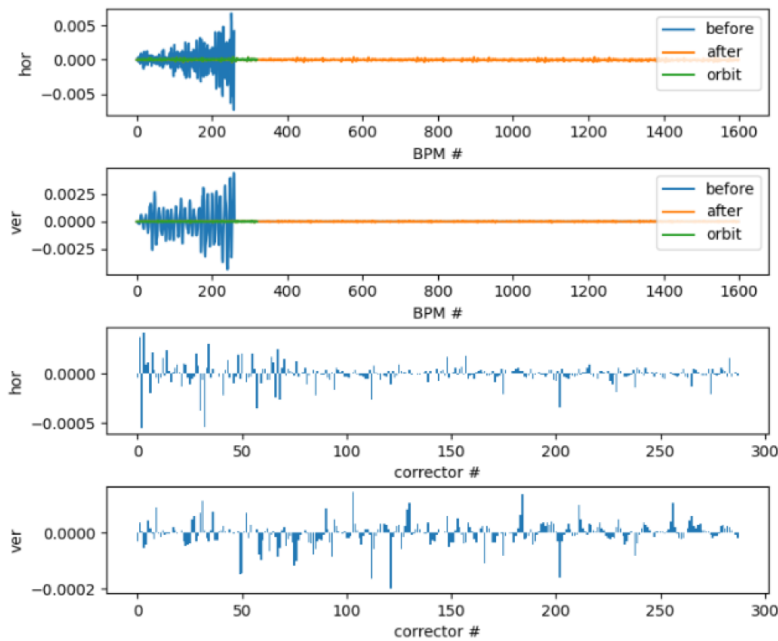


Figure 17: Trajectory correction to get first turns and beam accumulation

³⁵ S M Liuzzo and N Carmignani and A Franchi and T Perron and K B Scheidt and E Taurel and L Torino and S M White, "Preparation of the EBS beam commissioning", Journal of Physics: Conference Series, IOP Publishing, 10.1088/1742-6596/1350/1/012022, 2019

³⁶ Simone Liuzzo, Nicola Carmignani, Lee Carver, Laurent Farvacque, Thomas Perron, et al.. HMBA Optics Correction Experience at ESRF. *12th International Particle Accelerator Conference*, May 2021, Online, Brazil. pp.TUPAB048, [10.18429/JACoW-IPAC2021-TUPAB048](https://doi.org/10.18429/JACoW-IPAC2021-TUPAB048)

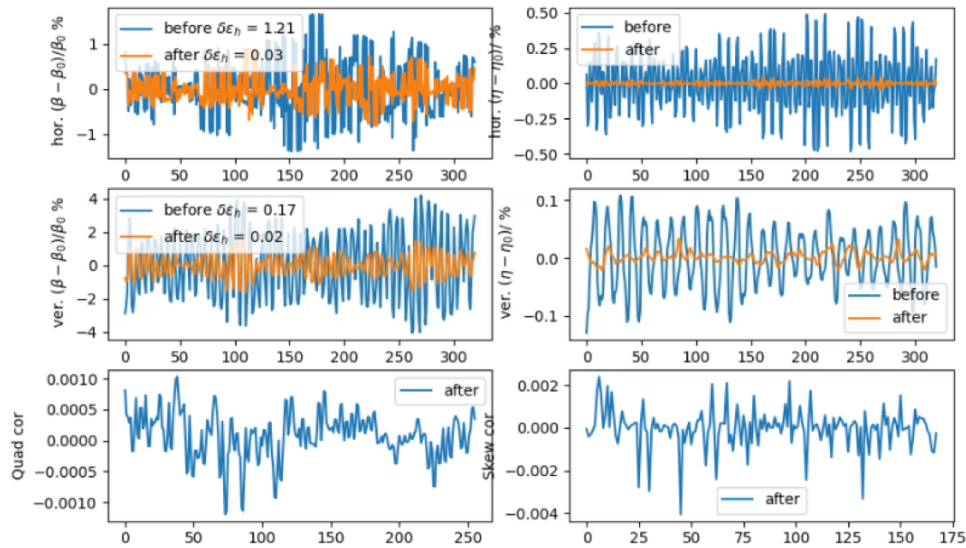


Figure 18: optics dispersion and coupling correction based on measured orbit response matrix fit.

In the near future also the following corrections will be added:

- BBA
- BBA from trajectory data
- NOECO³⁷
- tune from trajectory

These corrections may be done in any sequence and are fully tunable in all their parameters. A typical correction sequence executes the corrections in the order listed above and iterates a few times before considering the lattice converged.

Implementation and use of analytic formulas

Several steps of corrections require the computation of response matrices ahead (for example the response of orbit to a variation of each steerer magnet in the lattice). Those matrices are computed based on the design lattice and stored in files such to be available for individual parallel correction computations of each seed. These computations, even if done only once, may be rather long, in particular those necessary for the optics correction that require to compute the response of orbit at every steerer in both planes and for each normal and skew quadrupole in the lattice. Moreover in some cases it is necessary to update these matrices during the correction, thus multiplying the number of long computations.

³⁷ D.K. Olsson, Å Andersson, M. Sjöström, “Nonlinear optics from off-energy closed orbits”, Phys. Rev. Accel. Beams, 10.1103/PhysRevAccelBeams.23.102803

For this reason the code took advantage of recent analytic results³⁸ to make such computations as fast as possible.

In particular, the equations presented in ³⁹ are implemented by making use of tick magnets corrections. This was never done before, and proved to be crucial to make the analytic formulas work correctly.

An example of the formulas introduced for Tune Response is given below (simplest case). The equation on the first row corresponds to the thin magnet approximation, the one on the second row to thick magnet corrections. K is the quadrupole gradient, L its length and α , β , γ are the Twiss optics parameters.

$$\frac{\Delta Q}{\Delta K_j} = \frac{\beta_j}{4\pi}$$

$$\frac{\Delta Q}{\Delta K_j} = \frac{\frac{1}{2} \left[\beta_j + \frac{\gamma_j}{K_j} \right] + \frac{\sin(2\sqrt{K_j}L_j)}{4\sqrt{K_j}L_j} \left[\beta_j - \frac{\gamma_j}{K_j} \right] + \frac{\alpha_j}{2K_jL_j} [\cos(2\sqrt{K_j}L_j) - 1]}{4\pi}$$

The formulas are tested against their numeric equivalent and show extremely good agreement when including thick magnet corrections for steerers and quadrupoles.

In Figure 19 the numeric (reference) and analytic response matrices are compared

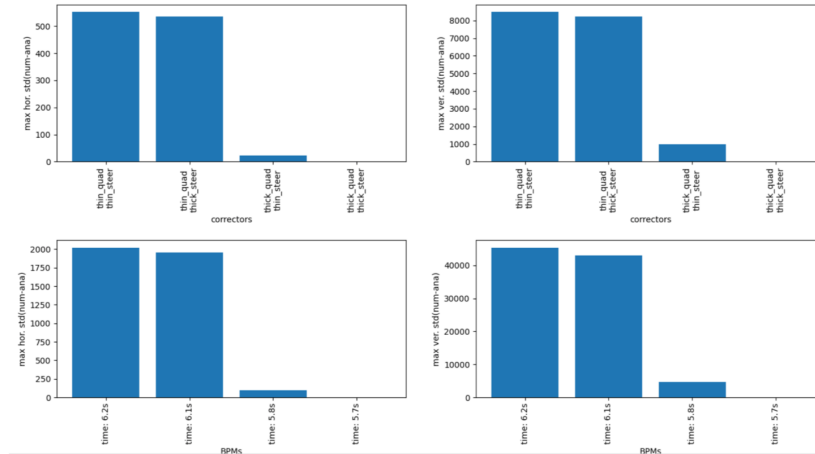


FIGURE 19: comparison of the residual difference between analytic and numeric response matrices in several cases: without thick magnets corrections, with thick steerers corrections, with thick quadrupole corrections and with tick steerers and quadrupole corrections.

³⁸ <https://arxiv.org/abs/1711.06589v2>

³⁹ <https://arxiv.org/abs/1711.06589v2>

The use of these equations allows to significantly speed up the computations. Several tests were performed showing a gain of a factor ~ 8 in speed for equal computing power conditions (see Figure 20).

Publication of the above results is foreseen at the next IPAC 2023 conference in Venice.

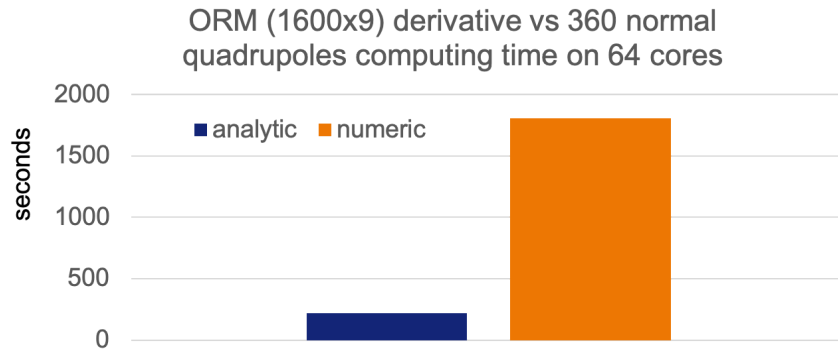


FIGURE 20: numeric and analytic computation speed for a derivative of orbit response matrix (1600 Beam position monitors, 8 steerers, 360 quadrupoles) run in parallel on a 64CPUs AMD EPYC 7543 3.5 GHz processor.

Typical output of commissioning simulations in pyAT

The typical results of a full commissioning simulation in pyAT performed with the code developed in the framework of the EURIZON project are presented in Figures 21 and 22 for the EBS lattice.

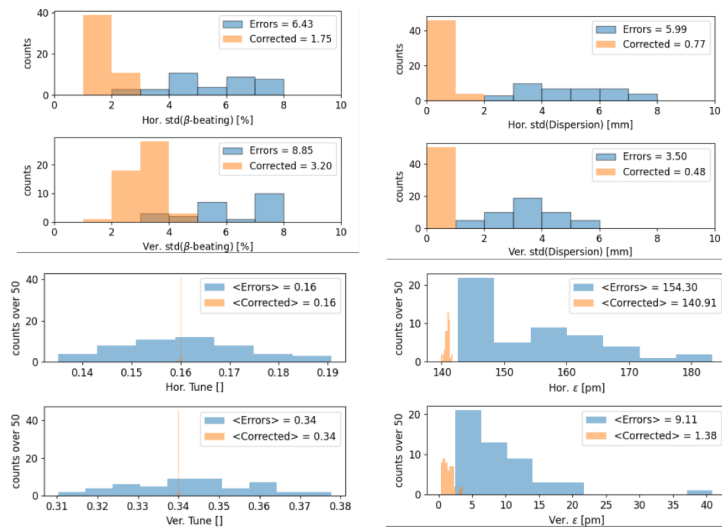


FIGURE 21: optics parameters before and after correction for commissioning simulations of the EBS lattice

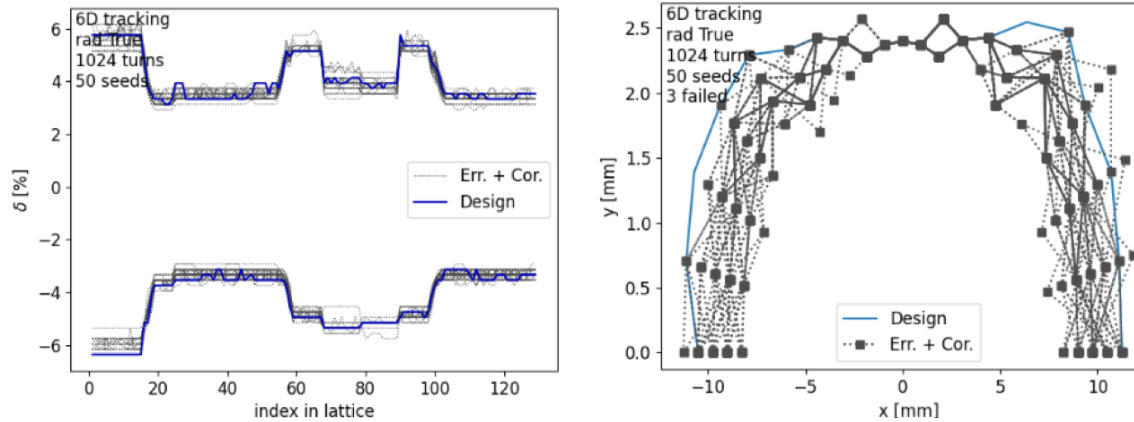


FIGURE 22: DA and MA after correction for commissioning simulations of the EBS lattice

The same software has presently been used for the EBS lattice⁴⁰, ESRF-DBA lattice⁴¹, for the FCC-ee⁴² collider lattice and for the PETRAIV lattice⁴³.

Several features are still under development and will be part of the next report:

- additional correction modules
- tests with other SR lattices
- extended errors, in particular large amplitude survey errors

⁴⁰ P. Raimondi, N. Carmignani, L.R. Carver, J. Chavanne, L. Farvacque, G. Le Bec, D. Martin, S.M. Liuzzo, T. Perron, S. White, “Commissioning of the hybrid multibend achromat lattice at the European Synchrotron Radiation Facility”, PhysRevAccelBeams.24.110701, 10.1103/PhysRevAccelBeams.24.110701

⁴¹ G. Chasman, K. Green and E.M. Rowe. “Preliminary design of a dedicated synchrotron radiation facility”, Technical report, United States, 1974

⁴² K.Oide, S. Aumon, T. Charles, D. El Khechen, D. Shatilov, T. Tydecks “Several Topics on Beam Dynamics in FCC-ee”, 62nd ICFA Advanced Beam Dynamics Workshop on High Luminosity Circular e+e- Colliders, 10.18429/JACoW-eeFACT2018-MOYAA01

⁴³ I. Agapov, R. Brinkmann, Y.-C. Chae, X. Gavalda, J. Keil, R. Wanzenberg, Rainer, “Lattice Design for PETRA IV: Towards a Diffraction-Limited Storage Ring”, 60th ICFA Advanced Beam Dynamics Workshop on Future Light Sources, 10.18429/JACoW-FLS2018-MOP1WB01, 2018



Future plans for pyAT developments

Due to the many ongoing upgrade programs, there is a growing need in the accelerator community to perform beam commissioning and errors specification simulations. In an effort to make the numerical tools available and ready to use in an existing well established environment we have plans to integrate the functionalities needed to perform these simulations in pyAT directly.

In this spirit, several developments are presently ongoing:

- build objects allowing to observe or vary arbitrary accelerator quantities and subsystems as present and available in real accelerator
- define a framework for lattice errors definition and management
- define a framework for lattice corrections

These basic bricks can be applied to accelerator design as well as operation and have to be thought of in such a way that they are flexible enough to be integrated in numerical tools with diverse applications. This would eventually allow us to switch back and forth from the simulation environment to the real accelerator but also from one machine to the other seamlessly and apply the same algorithms with minor adjustments.

Other activities related to the Task 4.1

Three visits took place and 2 are planned.

EBS restart visit in August 2022 with the participation of the members of the project to machine re-commissioning after the summer shut down.

A visit for machine dedicated time (MDT) on turn by turn data taking.

A visit for machines dedicated time on Vertical/Emittance and Lifetime optimizations.

13 meetings were organized and the relevant information and minutes are available online (<https://indico.esrf.fr/category/2/>).

2 visits are being planned in March and April 2022 for MDT time in PETRA-III



Appendix A

Provisional planning of a machine dedicated time on an Extremum Seeking algorithm for lifetime optimisation. It would be compared to the current ESRF lifetime optimisation, developed by N. Carmignani⁴⁴, which minimizes the machine losses using 24 sextupole knobs and 4 octupole knobs, each scanned one by one. The comparison criterion includes end lifetime and optimisation duration.

From the simulations conducted and detailed in Section “Lifetime optimizations using extremum seeker”, the Extremum Seeker algorithm best reacts with a limited number of knobs, even for the linear problematic of vertical emittance minimisation. Therefore, the ES adapted for losses minimisation would be tested both using all the knobs at once and using a partition of the knobs ensemble. In the latter, the ES would be run for each knob partition. To reduce the running time of the optimiser, the expected partitions are: four sets of seven knobs each, mixing all sextupoles and octupoles, or 4 sets of six sextupole knobs, and a set including all four octupole knobs. Since the knobs are considered to be independent, the order of apparition of the knobs between and within the sets is of no importance to the minimisation result.

MDT planning : ES lifetime optimisation

1. Set up the machine for a fair comparison
 - a. Save the SR magnet file
 - b. Remove sextupoles and octupole correction strengths, to cancel any previous optimisation/correction.
 - c. Correct orbit and tunes at low current. Ramp up to 200mA.
 - d. Save SRMagnet file (ring0)
2. Run the Extremum Seeking algorithm
 - a. all knobs at once,
 - i. Save a data file with start time and start lifetime.
 - ii. Scan the hyper parameters of the algorithm and register its response with selected knobs for post-processing.
 - iii. Save the hyper parameters
 - iv. Write the time down and end lifetime
 - v. Save all files and run data acquisition after each step
 - vi. Save a .mat with all sent correction strengths.
 - b. Splitted sets of knobs,
 - i. Repeat 2.a.i to 2.a.vi
3. Current ESRF lifetime optimisation
 - a. Restore ring0 by removing all corrections implemented by the ES. Orbit and tune correction.
 - b. Save a data file with start time and start lifetime.
 - c. Conduct standard lifetime optimisation script for all knobs used in the ES - in case not all possible knobs were used.
 - d. Save a data file with end time and end lifetime.
 - e. Save SRMagnet file.
 - f. Save a .mat with all optimized correction strengths.

⁴⁴ N.Carmignani et al. Online optimization of the ESRF SR. [10.18429/JACoW-IPAC2022-THPOPT001](https://doi.org/10.18429/JACoW-IPAC2022-THPOPT001)